PHYSICAL REVIEW B VOLUME 47, NUMBER 23 15 JUNE 1993-I

Interchain coupling and optical absorption in degenerate and nondegenerate polymers

J. A. Blackman and M. K. Sabra*
Department of Physics, University of Reading, Whiteknights, P.O. Box 220, Reading RG6 2AF, United Kingdom

(Received 17 December 1992)

We present a numerical study based on an extended Su-Schrieffer-Heeger model of the effects of interchain coupling on both degenerate and nondegenerate conjugated polymers. In particular, we study polaronic and bipolaronic excitations and examine their delocalization (spread over more than one chain) as a function of the coupling strength. It is shown that there is a discontinuous change in the degree of delocalization at a critical value of the coupling. We also study the influence of delocalization on the optical absorption and show that, in the polaron case, the relative strength of spectral lines in the absorption gap below the interband transitions is changed dramatically from the behavior predicted for independent chains.

I. INTRODUCTION

It is usually assumed that the electronic properties of conjugated polymers can be described in terms of the behavior of isolated chains. Using a Su-Schrieffer-Heeger[1,2] (SSH) type of parametrization, a typical intrachain hopping energy is 2–3 eV, while the interchain hopping is an order of magnitude or more smaller, perhaps 0.1 eV. At first sight, a single chain description would appear to be a reasonable approximation. There are, however, certain situations in which even small interchain coupling can have a significant effect as will be demonstrated in this paper.

There have been extensive discussions of the effect of interchain coupling, most of it focusing on *trans*-polyacetylene. The earlier work[3,4] employed a simple extension to the SSH model, and predicted an antiparallel ordering of the dimerization patterns on neighboring chains (double bonds on one chain adjacent to single bonds on its neighbor). Later experimental evidence[5] indicated, however, that it is the parallel ordering (like bonds on neighboring chains are adjacent) that actually occurs. Such preferred ordering can be incorporated into the extended SSH model if, for example, modulations are introduced into the interchain coupling.[6]

The effect of interchain coupling on polaronic and bipolaronic excitations is interesting and possibly quite important. For example, in the degenerate polymer, *trans*-polyacetylene, bipolarons are unstable and dissociate into a soliton and an antisoliton. The presence of interchain coupling provides a binding energy for the soliton-antisoliton pair and renders the bipolaron a stable excitation.[7] Another consequence of interchain coupling is the possibility that a polaron may become delocalized and no longer be confined to a single chain. The conditions for stability have been investigated.[8–10] It was found that delocalization occurs much more readily for parallel than for antiparallel ordering, and could quite realistically occur in practice, given the values of the interchain coupling to be expected in real systems.

Although estimates of the criteria for delocalization have been made, there have not been any studies that follow the behavior of a polaron as a continuous function of interchain coupling. Is there a critical value of the coupling at which delocalization occurs, or does the spread of the polaron over several chains increase gradually as the coupling increases? One of the purposes of the current work is to answer such questions, a task which it is necessary to perform numerically. The paper considers polarons (single injected electrons) and bipolarons (two added electrons) in both *trans*- and *cis*-polyacetylene. In the latter case energies can be scaled so as to yield good predictions for other nondegenerate polymers. Solitons are, of course, also of interest in *trans*-polyacetylene. We confine our attention here to polaronic excitations, however, because they have relevance for a wider range of polymers.

We give first, in Sec. II, a brief review of the previous work in this field. This is followed, in Sec. III, with a description of the numerical procedure employed in our work. The results are analyzed in Sec. IV, where it is shown that delocalization occurs discontinuously at a critical value of coupling. The discontinuity is larger for the polaron than for the bipolaron.

One way in which the behavior of electronic states in the band gap can manifest itself is through the optical-absorption spectrum. The optical absorption is calculated for a wide range of values of the interchain coupling and the results are described in Sec. V. The predicted behavior is very interesting, particularly for the case of a single injected electron. We find that absorption band intensity is extremely sensitive to the strength of the interchain interaction and, indeed, bands that have significant intensity in one regime of coupling strength may have essentially zero intensity in another regime. Interchain coupling in real systems is likely to be in the energy range at which the behavior deviates from that of isolated chains. The results described here, therefore, are potentially important for the interpretation of experimental data. A note about the relevant experimental background is given in the concluding section (VI).

0163-1829/93/47(23)/15437(12)/$06.00

II. CONSEQUENCES OF INTERCHAIN COUPLING—BACKGROUND

We consider a pair of chains of *trans*-polyacetylene, each one described by the static part of the SSH Hamiltonian[1,2]

$$H=-\sum_{j,n}[t_0+\alpha(u_{j,n}-u_{j,n+1})](c^\dagger_{j,n}c_{j,n+1}+\text{H.c.})+(K/2)\sum_{j,n}(u_{j,n}-u_{j,n+1})^2\ , \tag{1}$$

where $u_{j,n}$ is the displacement of a CH unit at site n on chain j ($j=1,2$) and $c^\dagger_{j,n}$ and $c_{j,n}$ are the corresponding π electron creation and annihilation operators. With a Peierls distortion, $u_{j,n}=(-1)^n u_0$, the electronic energy gap for a single chain is $E_g=2\Delta$, where $\Delta=4\alpha u_0$. Most of the previous work has been done also with just a pair of chains rather than a full three-dimensional environment. Because of size limitations inherent in numerical work, this is necessary for practical reasons in our case. Indications of how our results extrapolate to a full three-dimensional system will be given in the conclusion.

A. Antiparallel ordering

The simplest model to use for interchain hopping of the π electrons is

$$H'=-t_\perp\sum_n(c^\dagger_{1,n}c_{2,n}+c^\dagger_{2,n}c_{1,n})\ . \tag{2}$$

It was shown[3,4] that the total Hamiltonian $H+H'$ leads to an antiparallel configuration with double bonds in one chain adjacent to single bonds in the other. The bonding energy for this configuration is $t_\perp^2/\pi t_0$ per pair of CH groups and the energy gap is reduced to $E_g=2\Delta(1-t_\perp^2/8t_0^2)$.

There has been some interest in the behavior of soliton excitations in the presence of interchain coupling. A soliton is a demarcation between two different dimerization patterns and a single soliton is perfectly acceptable in an isolated chain. In the case of two coupled chains, however, solitons must exist as reasonably closely coupled pairs; otherwise, there will be an extensive length of the chains in which the energetically unfavorable parallel configuration occurs. The resulting confinement energy for solitons separated by a distance l can be calculated;[3,4] with either both solitons on the same chain or one on each chain, it is given, in the large l limit, by

$$E_{\text{conf}}=t_\perp^2 l/\pi t_0\ , \tag{3}$$

where l is measured in lattice spacings.

There are related implications for bipolaronic excitations. For an isolated chain, a bipolaron is unstable and dissociates into a soliton and an antisoliton. In the presence of interchain coupling, the arguments leading to Eq. (3) apply and dissociation is inhibited rendering the bipolaron stable. This was investigated earlier[7] by numerical methods. Regarding a bipolaron as a pair of coupled solitons, we found that, for typical values of the parameters, the stable soliton separation was about 15–20 lattice spacings. The equilibrium separation is determined by a balance between the confinement energy of Eq. (3), which is independent of the charge state of the solitons, and a repulsive (for the charged case) soliton overlap energy that decays exponentially with l.

Interchain coupling does not alter the behavior of a polaron appreciably because it is stable even on a single chain. Another possible consequence of interchain coupling is the spread of the wave function associated with the excitation onto the second chain and, if the interaction is strong enough, there could be complete delocalization. For the model of Eq. (2) this turns out to occur only for very large values of $t_\perp$, and it is safe to say that, in practical terms, the model does not predict delocalization over the two chains.

B. Parallel ordering

There is experimental evidence[5] that the antiparallel configuration is not the one that actually occurs—rather, the results point to parallel dimerization patterns on the two chains. Baeriswyl and Maki[6] showed that this behavior can be easily incorporated into a phenomenological SSH-type theory if minor changes are made to the Hamiltonian of Eq. (2). They wrote the interchain coupling in the following oscillatory form:

$$H'=-\sum_n[t_1+(-1)^n t_2](c^\dagger_{1,n}c_{2,n}+c^\dagger_{2,n}c_{1,n})\ , \tag{4}$$

and demonstrated that parallel ordering is favored energetically if $t_2>t_1$. The model in Eq. (4) is a plausible one given the three-dimensional (3D) structure of polyacetylene[11,12] with the polymer chains oriented with their planes at an angle to each other and CH units in neighboring chains at distances from each other that alternate in magnitude at successive sites along the direction of the chains. Total-energy calculations for possible 3D configurations have been made by Jeyadev[13] and Stafström.[14]

The bonding energy for the Hamiltonian of Eq. (4) is $(t_2^2/\pi t_0)\ln(8t_0/\Delta)$ per pair of CH units. The energy gap in this case is $E_g=2(\Delta^2+t_2^2)^{1/2}-2t_1$. Again, we find that solitons are confined in order to avoid a long length of chain being, in this case, in the energetically unfavorable antiparallel configuration. In the large l limit the confinement energy is given by[6,8]

$$E_{\text{conf}}=(t_2^2-t_1^2)l/\pi t_0\ . \tag{5}$$

As in the previous case this energy stabilizes the bipolaron against dissociation into free solitons.

There is a vital difference between the parallel and the antiparallel cases which has implications for delocalization. If there is an excitation on each chain, then the overlap of the electronic wave functions causes a splitting of the gap states. The overlap is essentially zero for antiparallel ordering while, for parallel ordering, an additional binding energy per charge of the order of t_1 results. A consequence of this is the possibility that excitations will spread over two chains rather than be localized on one. An analysis of the conditions for stability has been carried out by Baeriswyl and Maki,[8] Gartstein and Zakhidov,[9,10] and Emin.[15]

We can make the following argument about the stability of the doubly charged bipolaron: if the bipolaron is localized on a single chain, then it has cost energy $2E_s$ to create, where[2,16] $E_s=2\Delta/\pi$. If the two charges are, alternatively, spread over the two chains then, in the absence of interchain coupling, they would reside in polaron states, one per chain. The energy of the formation is $2E_p$, where[2] $E_p=\sqrt{2}E_s$. Since $2E_s<2E_p$, a doubly charged bipolaron on one chain is energetically preferred to singly charged polarons on two chains. With interchain coupling, however, an energy bonus favoring delocalization is a special feature of parallel alignment; the effect reduces the formation energy for an excitation spread over two chains to $2E_p-2t_1$, which gives, as a criterion for delocalization, $2E_p-2t_1<2E_s$, or

$$t_1>2(\sqrt{2}-1)\Delta/\pi=0.264\Delta\ . \tag{6}$$

An analogous argument for the case of a singly charged excitation leads to the following delocalization criterion:

$$t_1>2[4\sin(\pi/8)-\sqrt{2}]\Delta/\pi=0.074\Delta\ . \tag{7}$$

Baeriswyl and Maki[8] give the analysis for the full 3D system in which each chain has four neighbors. The physical arguments are essentially those that have just been presented, but the numerical factors on the right-hand sides of Eqs. (5) and (6) are replaced by 0.091 and 0.025, respectively. The important point to note is the rather small values of t_1 required for delocalization to occur—smaller than 0.1 eV (for typical values of Δ) and, in the case of a single injected electron, considerably smaller than that. Delocalization is likely to be important, therefore, for real systems.

The purpose of the present paper is to study the delocalization process in more detail and, in particular, to examine whether it occurs discontinuously at a critical value of the coupling. The method used is a numerical one and the procedure is described first.

III. NUMERICAL PROCEDURE

Analytic calculations, usually based on the continuum model,[16] are only possible for certain special limits. Using numerical methods, however, it is possible to follow the electron delocalization as a function of the strength of the interchain coupling. We use the Hamiltonian $H+H'$ of Eqs. (1) and (4), which is diagonalized directly, and the displacements $u_{j,n}$ are varied until an energy minimum is found. Earlier we found,[7] with chains each of length N units, that $N=128$ is long enough to eliminate any size dependence in the features we wish to study. Periodic boundary conditions are used to minimize finite-size effects.

The procedure is to start with a set of trial displacements $\{u_{j,n}\}$ and vary these until a minimum energy state is found. We notice that only the differences $U_{j,n}=u_{j,n}-u_{j,n+1}$ occur in Eqs. (1) and (4) and that there are only $N-1$ independent variables associated with each chain. For a particular frozen-in configuration $\{U_{j,n}\}$, the Hamiltonian $H+H'$ can be diagonalized to give eigenstates $|\lambda\rangle$, with

$$|\lambda\rangle=\sum_{j,n}a_{j,n}^{\lambda}|j,n\rangle\ . \tag{8}$$

The change in energy, ΔE, under small displacements $U_{j,n}\to U_{j,n}+\delta U_{j,n}$ can then be calculated by second-order perturbation theory

$$\Delta E=(K/2)\sum_{j,n}(2U_{j,n}\delta U_{j,n}+\delta U_{j,n}^2)-2\alpha\sum_{j,n}\delta U_{j,n}\sum_{\lambda}a_{j,n}^{\lambda}a_{j,n+1}^{\lambda}$$
$$+\alpha^2\sum_{j,n}\sum_{i,m}\delta U_{j,n}\delta U_{i,m}\sum_{\lambda}\sum_{\mu}(a_{j,n}^{\lambda}a_{j,n+1}^{\mu}+a_{j,n+1}^{\lambda}a_{j,n}^{\mu})(a_{i,m}^{\lambda}a_{i,m+1}^{\mu}+a_{i,m+1}^{\lambda}a_{i,m}^{\mu})(E_\lambda-E_\mu)^{-1}\ , \tag{9}$$

where the μ summation is over all $2N$ electronic states and the λ summation is over only occupied states. For the situations considered, the lowest N states are doubly occupied, while the $(N+1)$th state is either singly (one injected electron) or doubly (two injected electrons) occupied. Schematically, Eq. (9) can be written

$$\Delta E=\sum_{j,n}A_{j,n}\delta U_{j,n}+\sum_{j,n}\sum_{i,m}B_{j,n;i,m}\,\delta U_{j,n}\delta U_{i,m}\ , \tag{10}$$

and the minimization occurs with $\delta U=(2B)^{-1}A$. Because we use periodic boundary conditions, there are additional quite complicated terms in Eq. (9) which are not shown here explicitly, but were included in the calculations.

Three types of starting configuration were employed in the iterations:

$$u_{j,n}=(-1)^n u_0\ , \tag{11}$$

$$u_{j,n}=u_0+(u_0/\sqrt{2})\{\tanh[(x-x_0)/\sqrt{2}\xi]-\tanh[(x+x_0)/\sqrt{2}\xi]\}\ , \tag{12}$$

$$u_{j,n}=(-1)^n u_0\begin{cases}-\tanh[(n-n_1)/\xi]\ , & n<n_0\\ \tanh[(n-n_2)/\xi]\ , & n\ge n_0\ .\end{cases} \tag{13}$$

Equation (11), of course, represents a pristine chain, while Eqs. (12) and (13) are, respectively, canonical forms for the polaron and bipolaron (conceived as a soliton-antisoliton pair). In Eq. (13), $n_0=(n_1+n_2)/2$, the midpoint between the soliton and the antisoliton. Optimum values for the various parameters were found empirically for each situation.

It was recognized that more than one energy minimum was possible. To investigate this, two different starting configurations were used for each set of interchain coupling parameters: in one, the excitation was entirely confined to one chain [Eq. (12) or (13) was used for chain $j=1$ for one or two injected electrons, while chain $j=2$ was described by Eq. (11)]; in the other, the excitation was equally distributed between the two chains [Eq. (12) was used for both chains irrespective of the number of injected electrons]. In the latter case, slightly different starting parameters were used for each chain to avoid the possibility of getting stuck on an energy maximum. Two iterations using the algorithm described were usually sufficient to ensure convergence to a configuration of minimum energy. The precise functional forms of the three equations is not important. Simply, they represent convenient localized and delocalized starting points for the iterative algorithm.

We are interested in monitoring the delocalization of the electron(s) as a function of interchain coupling. If the expansion coefficients for a gap-state wave function in Eq. (8) are $a_{j,n}^{g}$, then the weight on chain j is

$$W_j=\sum_n a_{j,n}^{g2} \; . \tag{14}$$

W_j will vary from 1 (or 0) when the electron is localized on one chain to 0.5 as the electron becomes delocalized. A convenient parameter to describe the degree of localization is

$$\Lambda=|W_1-W_2| \; . \tag{15}$$

Λ is equal to 1 when the electron(s) in the polaron or bipolaron state is (are) completely localized on one chain and it is zero when equally distributed between the two chains.

Various sets of parameters are commonly used in model calculations. In the numerical results that follow, the set we employed for a single chain (see Ref. 2) is $t_0=2.5$ eV, $\alpha=4.1$ eV Å^{-1}, $K=21$ eV Å^{-2}; with these we obtain $u_0=0.0397$ Å from energy minimization and thus $\Delta=0.651$ eV and an energy gap of 1.3 eV. A range of values of the interchain coupling t_1 is explored. Throughout we take $t_2=1.5t_1$; this ensures parallel ordering and, apart from that, the actual results are expected to be relatively insensitive to the precise value of t_2. The values chosen for the parameters are not too important in themselves because a plausible energy scaling can be done to extrapolate the results to alternative sets of parameters. Because of this we express our results in terms of dimensionless variables.

A simple extension to the numerical procedure can be developed for *cis*-polyacetylene. The parametrization used for this system is described in Sec. IV C.

IV. RESULTS

A. *Trans*-polyacetylene ($2N+1$ electrons)

There are $2N$ sites in our two-chain model. For a neutral system, the total energy is obtained by diagonalizing the Hamiltonian and calculating the total energy of $2N$ electrons in the lowest N eigenstates. We consider here a system of $2N+1$ electrons; the addition of a single hole ($2N-1$ electrons) is, of course, identical energetically because of the symmetry of energy levels about zero.

We examine first the delocalization parameter Λ as a function of t_1. Because the delocalization conditions are expected to scale as Δ [see Eq. (7)], we plot Λ as a function of t_1/Δ in Fig. 1. As stated, we consider two starting points for iterations to a minimum energy configuration: in one the electron is localized on a single chain [Eqs. (11) and (12)], while in the other [Eq. (12)] there is complete delocalization. For certain (lower) values of t_1 there are two minimum energy configurations, the actual one reached after iteration depending on the starting point. For other (higher) values of t_1, the final minimum energy configuration is independent of the starting point. The global minimum is shown by the full curve in Fig. 1; metastable minima are indicated by the broken curves. It can be seen that there is a critical value t_{1c} of the interchain coupling at which the delocalization parameter Λ changes abruptly from a finite value (about 0.5) to zero, and this can reasonably be said to mark the transition. The value $t_{1c}=0.127\Delta$ is somewhat higher than the calculated value in Eq. (7), but any discrepancy is essentially due to inherent imprecision in the definition of a critical value in the derivation of Eq. (7).

The dependence of the positions of the band edge and gap state on the interchain coupling are plotted in Fig. 2. The band edge, as expected, follows the predicted behavior close to $(\Delta^2+t_2^2)^{1/2}-t_1$, approximately linear in t_1 because t_2 is much smaller than Δ over the region displayed. There is a very small discontinuity in the position of the band edge at t_{1c}. The gap state is at $\Delta/\sqrt{2}$ for $t_1=0$ as is expected for a polaron on a single chain, and its position increases slowly until t_{1c} when, after a discontinuous change, it falls in energy in parallel with the band edge. The observed behavior is as one might expect. The linear (in t_1) shift in the band edge arises because there is

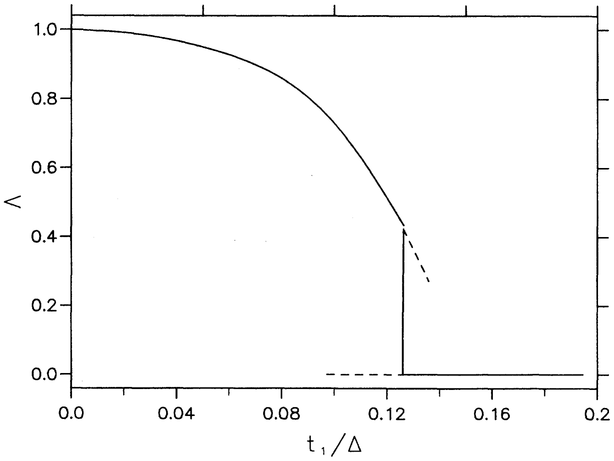

FIG. 1. *Trans*-polyacetylene; $2N+1$ electrons. The delocalization parameter Λ as a function of t_1 (in units of Δ). The solid line represents the lowest of the minimum energy configurations; the broken line indicates the metastable energy minimum.

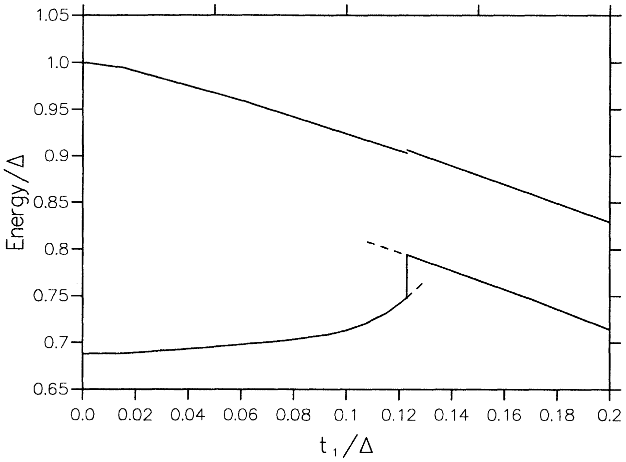

FIG. 2. *Trans*-polyacetylene; $2N+1$ electrons. Band-edge (upper curve) and gap-state positions as a function of t_1 (all energies in units of Δ). Broken lines indicate gap-state positions of metastable configurations of Fig. 1.

a degeneracy between the band states of the two chains which is split by the interchain coupling (a similar degeneracy between the soliton states, one on each chain, and a consequent linear splitting, was discussed in Sec. II B). In the case of the polaron states on a single chain, there is no degeneracy involved and any shift will be in second order. It will thus be of order t_1^2/Δ and is much smaller than the shift in the band edge as is observed.

The actual displacements $|U_{jn}|$ (where $U_{j,n} = u_{j,n} - u_{j,n+1}$) of the two chains for a range of values of t_1 are shown in Fig. 3. For $t_1 = 0.169\Delta$ (chain curve), where complete delocalization has taken place, the displacements of the two chains are identical. The broken curve shows displacements for a value of t_1 just below t_{1c}.

The projection of a gap-state wave function on each site of the chains is displayed in Fig. 4 for the same set of values of t_1. The gap state becomes more spatially extended along the chain as delocalization increases.

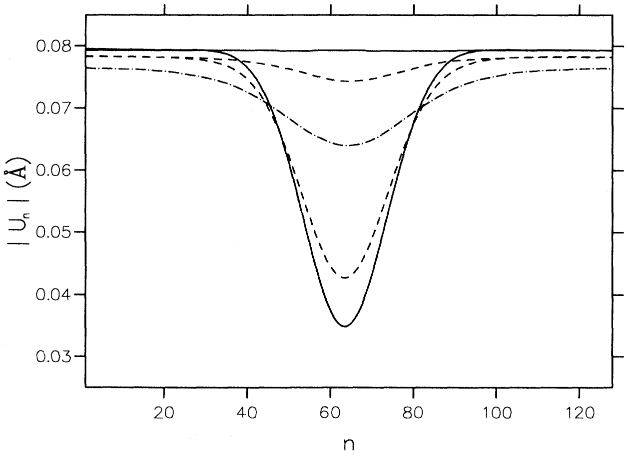

FIG. 3. *Trans*-polyacetylene; $2N+1$ electrons. Displacements $|U_n|$ for chains 1 and 2 for three different values of t_1: $t_1/\Delta = 0.015$ (full line); 0.108 (broken line); 0.169 (chain line).

We also record the total energy of the system as a function of the interchain coupling in Fig. 5. The energy $E(t_1)$, with $t_2 = 1.5t_1$, is calculated as described. The quantity plotted in the figure is ΔE, defined as

$$\Delta E = E(t_1) - E(t_1=0) + (N t_2^2/\pi t_0)\ln(8t_0/\Delta) , \qquad (16)$$

where the last term is the interchain bonding energy for pristine chains. ΔE is a measure of the contribution from the interchain coupling to the binding energy of the nonlinear excitation associated with the gap state. It can be seen that, once delocalization has taken place, ΔE varies roughly linearly in t_1 as has been suggested by the arguments of Sec. II B.

B. *Trans*-polyacetylene ($2N+2$ electrons)

In the absence of interchain coupling, a bipolaron is unstable, dissociating into a pair of singly charged solitons. Interchain coupling stabilizes the bipolaron against dissociation in the case of parallel ordering just as it does in the antiparallel case investigated earlier.[7] Numerical calculations were performed for a system of $2N+2$ electrons, and we consider first the delocalization parameter Λ which is shown as a function of t_1 in Fig. 6. Again, localized and delocalized initial configurations were used to start the iterative algorithm. Let us consider first the case of two decoupled chains ($t_1=0$). There are two solutions (generated numerically from the two different starting configurations). The $\Lambda=0$ solution corresponds to two decoupled polarons (one added electron in each chain), and the $\Lambda=1$ case corresponds to a bipolaron in an isolated chain. In the latter case, the bipolaron is, of course, unstable, and dissociates into two solitons (in practice separated by half the chain length because of its finite size in numerical calculations). Since $2E_s < 2E_p$, the $\Lambda=1$ solution has the lower energy. As t_1 is increased from zero, it can be seen that, for two added electrons, the delocalization occurs almost continuously as a function of t_1. There is, in fact, a small discontinuity at $t_1 = 0.40\Delta$ where Λ changes from a finite value (about 0.1) to zero. We define this as the critical value t_{1c} for delocalization. Again, metastable solutions are shown by broken lines. The broken line at $\Lambda=0$, of course, can be continued back to $t_1=0$ and the upper broken curve can be extended down to $\Lambda=0$ so that a single minimum energy solution exists for t_1 greater than about 0.44Δ. The critical value of t_1 is considerably higher than the value of Eq. (6). This is largely a matter of definitions. The discontinuity in Fig. 6, which defines our t_{1c}, occurs at a very small value of the delocalization parameter (~ 0.1) while, at the values of t_1 given by the Eq. (6) definition, there is intermediate delocalization ($\Lambda \sim 0.6$).

The band edge and position of the gap state are displayed in Fig. 7. As in Fig. 2, the band edge moves almost linearly with t_1. In the absence of interchain coupling, the gap state is, of course, at the center of the band gap being a degenerate level corresponding to a dissociated soliton-antisoliton pair. It moves away from the center linearly with t_1 as a result of the splitting of the

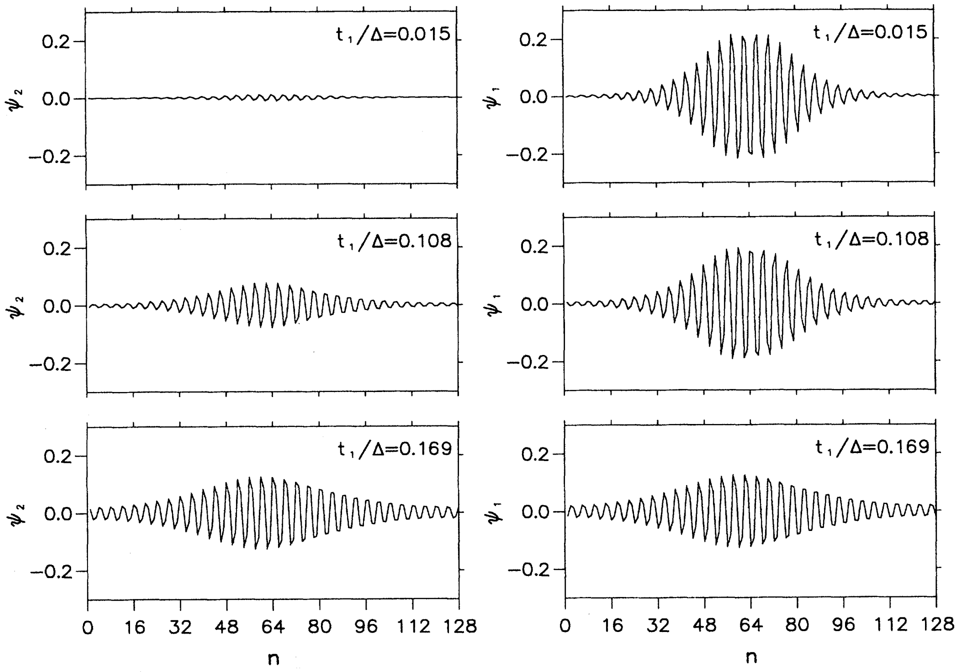

FIG. 4. *Trans*-polyacetylene; $2N+1$ electrons. Projection of wave functions of the upper gap state onto chain 1 (right) and chain 2 (left) for three values of t_1.

degeneracy. The displacements $|U_{j,n}|$ for three values of t_1 are shown in Fig. 8. Some small asymmetry in the displacements of the two chains is apparent at intermediate coupling.

The projection of a gap-state wave function is shown in Fig. 9. The change from a bipolaronic form to something more polaronic as coupling is increased is apparent.

As long as relatively little delocalization has occurred (small t_1), the bipolaron can be considered as a coupled soliton-antisoliton pair, and we can measure its size l in terms of the separation between the points at which $|U_n|$ are zero (see Fig. 8). Increasing t_1 results in larger binding for the polaron and a reduced l. The behavior can be understood in terms of a system energy written phenomenologically as

$$E=E_0+A\exp(-l/\rho)+Bt_1^2+Ct_1^2 l\ , \qquad (17)$$

where E_0 is the energy of the two chains in the presence of a dissociated soliton-antisoliton pair; the second term arises from the overlap of the soliton and antisoliton wave functions; the third term represents the energy arising from interchain coupling; and the fourth accounts for the additional energy that results from the antiparallel configuration of length l. If the energy E is minimized with respect to l, the following relation between l and t_1

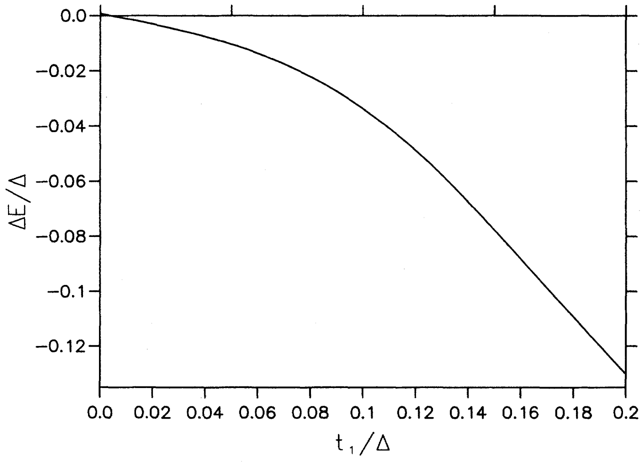

FIG. 5. *Trans*-polyacetylene; $2N+1$ electrons. Energy ΔE [from Eq. (16)] against t_1, both in units of Δ.

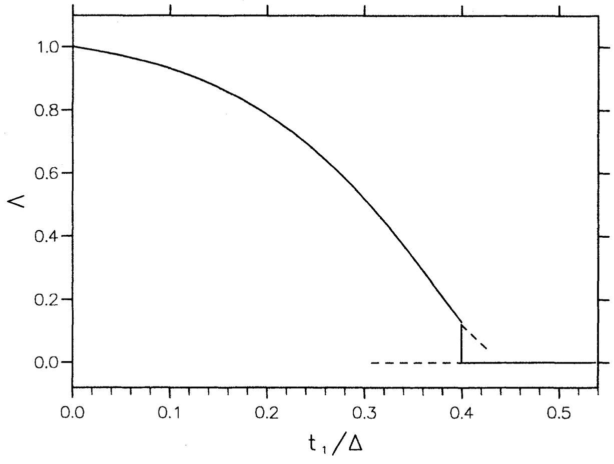

FIG. 6. *Trans*-polyacetylene; $2N+2$ electrons. The delocalization parameter Λ as a function of t_1 (in units of Δ). The solid line represents the lowest of the minimum energy configurations; the broken line indicates the metastable energy minimum.

is obtained:

$$l=\rho[\ln(A/C\rho)-2\ln(t_1)]\ . \tag{18}$$

The functional dependence is confirmed in Fig. 10, from which a value of ρ of 3.5 lattice spacings can be extracted.

C. *Cis*-polyacetylene ($2N+1$ electrons)

An additional term can be added to the SSH Hamiltonian[17] to model the lifting of the ground-state degeneracy in *cis*-polyacetylene. Later, a more refined version was introduced by Wang, Su, and Martino,[18] and that is the one we use here. Equation (1) for a single chain is replaced by

$$H=-\sum_{j,n}[t_{01}+\alpha_1(u_{j,2n}-u_{j,2n+1})](c^{\dagger}_{j,2n+1}c_{j,2n}+\text{H.c.})-\sum_{j,n}[t_{02}+\alpha_2(u_{j,2n+1}-u_{j,2n+2})](c^{\dagger}_{j,2n+2}c_{j,2n+1}+\text{H.c.})$$
$$+(K/2)\sum_{j,n}(u_{j,n}-u_{j,n+1})^2 \tag{19}$$

The one-electron potential is modulated so that there is an energy gap even in the absence of lattice distortion. We consider this Hamiltonian with interchain coupling given by Eq. (4) to investigate electron delocalization for *cis*-polyacetylene. The energies of polaron and bipolaron excitations can only be obtained numerically so it is not possible to derive criteria for delocalization like Eqs. (6) and (7) analytically.

Minimum energy configurations were found by numerical iteration as previously described. The results of Sec. III are trivially extended for the nondegenerate polymer. The following values[18] for the parameters in Eq. (19) were used: $t_{01}=2.51$ eV, $t_{02}=2.49$ eV, $\alpha_1=4.47$ eV Å^{-1}, $\alpha_2=4.43$ eV Å^{-1}, $K=21$ eV Å^{-2}.

When energies are scaled by the width of the band gap the delocalization behavior is essentially indistinguishable from the *trans*-polyacetylene case. In particular, the delocalization parameter Λ shows dependence on interchain coupling that is virtually identical to Fig. 1. With Δ now representing the half-band-gap of the pristine *cis*-polyacetylene single chain (1.02 eV for the parameters used), the discontinuity again occurs at a value of t_1/Δ of just below 0.13. The other properties may similarly be obtained from the *trans*-polyacetylene results if energies are appropriately scaled. They are not repeated here. Other nondegenerate polymers can also be represented by Eq. (19), and the ensuing discussion applies if appropriate values of parameters and energy scale Δ are used.

The $2N+2$ electron problem appears to differ considerably from the *trans*-polyacetylene case. In particular, delocalization requires much higher values of interchain coupling to be at all appreciable. For example, for a t_1/Δ of about 0.4, Λ has decreased only to 0.7. Clearly, the effect is not likely to be significant in practical situations and we do not explore it further. There is, of course, for bipolarons in an isolated chain, a fundamental difference between the *trans*- and *cis*- cases that does not exist for the polaron. The bipolaron is stable in *cis*-$(\mathrm{CH})_x$ while in *trans*-$(\mathrm{CH})_x$ it dissociates into a soliton-antisoliton pair. The size of the bipolaron in *cis*-polyacetylene changes little over the range of t_1 examined.

V. OPTICAL ABSORPTION

A convenient way to study the behavior of states within the energy gap is via optical-absorption measure-

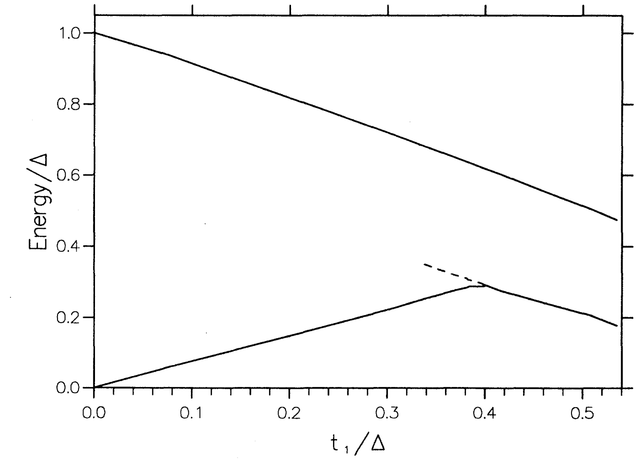

FIG. 7. *Trans*-polyacetylene; $2N+2$ electrons. Band-edge (upper curve) and gap-state positions as a function of t_1 (all energies in units of Δ). Broken lines indicate gap-state positions of metastable configurations of Fig. 6.

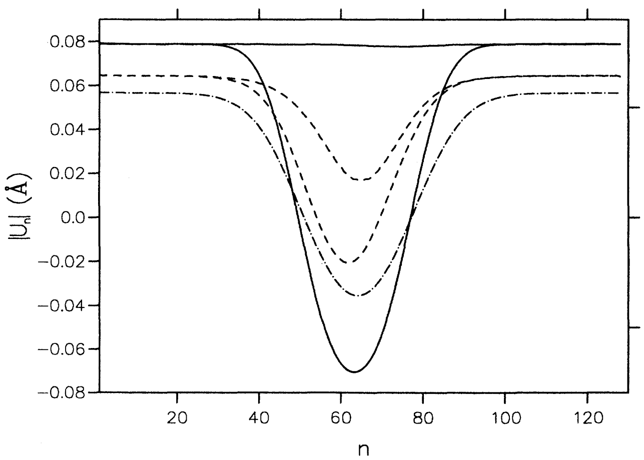

FIG. 8. *Trans*-polyacetylene; $2N+2$ electrons. Displacements $|U_n|$ for chains 1 and 2 for three different values of t_1: $t_1/\Delta=0.077$ (full line); 0.384 (broken line); 0.461 (chain line).

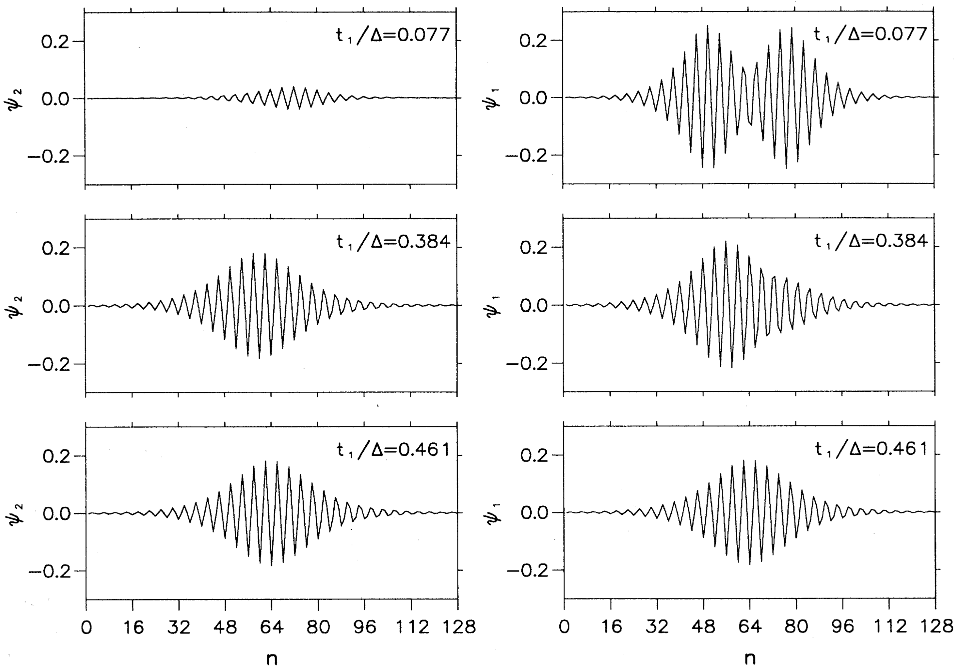

FIG. 9. *Trans*-polyacetylene; $2N+2$ electrons. Projection of wave functions of the upper gap state onto chain 1 (right) and chain 2 (left) for three values of t_1.

ments. The optical absorption $\alpha(\omega)$ is given by the standard golden rule approximation,

$$\alpha(\omega)=(4\pi^2Ne^2/m^2c\hbar\omega)\sum_{\lambda}|P_{0\lambda}|^2\delta(\omega-\omega_\lambda)\ , \tag{20}$$

where N is the number of polymer molecules per unit volume, λ denotes an excited state of the system, and the subscript 0 indicates the ground state. It is assumed that light is polarized along the chain direction and so the momentum P is in that direction also. Absorption associated with perpendicular polarization is more than an order of magnitude smaller[19] and is not considered in these calculations. All transitions, with the exception of those involving the upper gap state in the case of a single added electron, carry a statistical weight 2 because of the spin states. Transitions which take place from or to a singly occupied gap state have a weight of 1.

Within a tight binding formalism (such as the SSH model), the polarization operator X is written[20]

$$X=\sum_{j,n}X_{j,n}c_{j,n}^{\dagger}c_{j,n}\ , \tag{21}$$

where $X_{j,n}$ is the position of the nth C atom on the jth chain. The conjugate momentum P is obtained from

$$P=(im/\hbar)[H,X]\ , \tag{22}$$

which, using Eq. (1), leads to

$$P=(im/\hbar)\sum_{j,n,\pm}t_{j,n}^{\pm}X_{j,n}^{\pm}c_{j,n}^{\dagger}c_{j,n\pm1}\ , \tag{23}$$

where

$$t_{j,n}^{\pm}=t_0+\alpha(u_{j,n}-u_{j,n\pm1})\ \text{and}\ X_{j,n}^{\pm}=[X_{j,n}-X_{j,n\pm1}]\ .$$

Then, from Eq. (20)

$$\alpha(\omega)=(4\pi^2Ne^2/c\hbar^3\omega)\sum_{\lambda}\delta(\omega-\omega_\lambda)\left|\sum_{j,n,\pm}t_{j,n}^{\pm}X_{j,n}^{\pm}\langle 0|j,n\rangle\langle j,n\pm1|\lambda\rangle\right|^2\ . \tag{24}$$

There are no contributions to $\alpha(\omega)$ from the interchain coupling as long as $X_{j,n}$ is independent of j, which it is to within a few percent. From Eq. (22), it is also straightforward to obtain the sum rule

$$\alpha\equiv\int\alpha(\omega)d\omega$$

$$=(2\pi^2Ne^2/\hbar^2c)\sum_{j,n\pm}t_{j,n}^{\pm}(X_{j,n}^{\pm})^2\langle 0|j,n\rangle\langle j,n\pm1|0\rangle\ . \tag{25}$$

If the displacement arising from the Peierls distortion can be neglected in comparison with the interatomic separation a then, in the absence of interchain coupling,

$$\alpha=(2\pi^2Ne^2/\hbar^2c)a^2E_{\text{el}}\ , \tag{26}$$

where E_{el} is the electronic contribution to the ground-state energy. A departure from Eq. (26) occurs when interchain coupling contributes significantly to E_{el}.

We distinguish five different contributions to the absorption of Eq. (25),

$$\alpha=\alpha_{\text{IB}}+\alpha_1+\alpha_2+\alpha_3+\alpha_4\ . \tag{27}$$

Referring to the valence band, the conduction band, and the lower and upper gap states as V, C, G_L, and G_U, respectively, the five contributions arise from the following single-particle excitations: α_{IB} (interband, $V\rightarrow C$); α_1

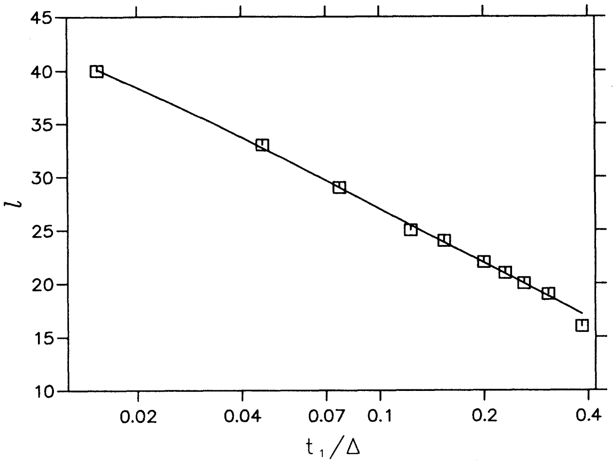

FIG. 10. *Trans*-polyacetylene; $2N+2$ electrons. "Size" of the bipolaron l as a function of interchain coupling.

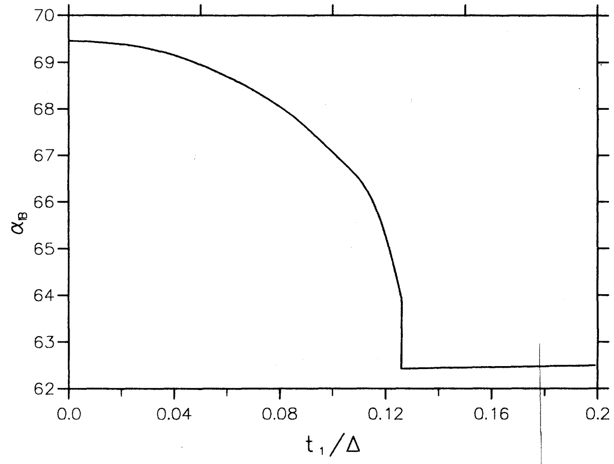

FIG. 12. *Trans*-polyacetylene; $2N+1$ electrons. Interband contribution to absorption, α_{IB}, as a function of t_1. Absorption is in arbitrary units.

$(G_L \rightarrow G_U)$; α_2 $(G_U \rightarrow C)$; α_3 $(G_L \rightarrow C)$; α_4 $(V \rightarrow G_U)$. The weights for the five cases arising from the spin states and differing occupancies of G_U are, respectively, 2, 1, 1, 2, 1 for the single injected electron case and 2, 0, 2, 2, 0 for two added electrons. Where we wish to distinguish the contributions to $\alpha(\omega)$ of Eq. (24), the notation $\alpha_{\text{IB}}(\omega)$, $\alpha_1(\omega)$, $\alpha_2(\omega)$, $\alpha_3(\omega)$, $\alpha_4(\omega)$ will be used. Because of the symmetry of the SSH Hamiltonian α_3 and α_4 are equivalent apart from the weighting factor. Where it is convenient to group together the contributions involving gap states, the following notation is used:

$$\alpha' = \alpha_1 + \alpha_2 + \alpha_3 + \alpha_4 \; . \tag{28}$$

A. *Trans*-polyacelylene ($2N+1$ electrons)

We consider the case of a single injected electron first and calculate the effect of the polaron delocalization on the optical absorption. $\alpha_1(\omega)$ appears as a sharp line in the gap and below it, deep in the gap, $\alpha_2(\omega)$ occurs as a narrow band. For transitions contributing to $\alpha_3(\omega)+\alpha_4(\omega)$, there is an absorption edge between the position of $\alpha_1(\omega)$ and the edge for interband transitions. The positions of the absorption edges are immediately obtainable from Fig. 2 and they are shown as a function of t_1 in Fig. 11. The interband absorption α_{IB} is displayed in Fig. 12, and the components arising from transitions involving gap states are shown in Fig. 13. The α_3 component (not shown explicitly) is just double α_4.

The optical absorption for a single chain has been calculated by a number of authors.[21,22] It is useful to make the connection between our calculations and the earlier work by examining the independent chain $(t_1 \rightarrow 0)$ limit in Fig. 13. It is seen that the absorption components α_1 and α_2 are of a similar magnitude while α_4 (and α_3) is almost zero. This is to be compared with Fig. 6 of Fesser,

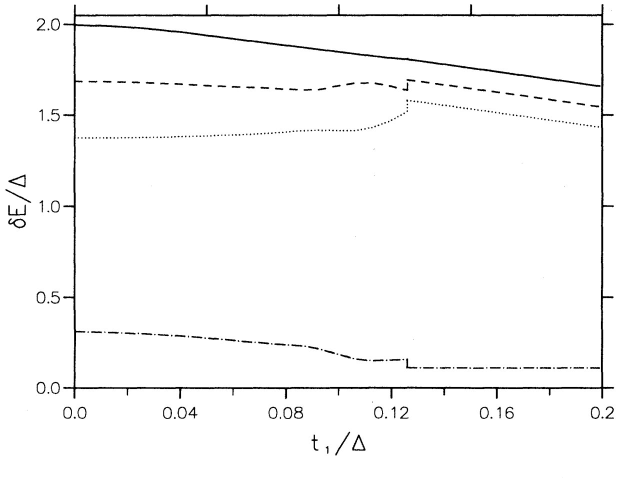

FIG. 11. *Trans*-polyacetylene; $2N+1$ electrons. Position of the absorption edges δE in units of Δ from the various categories of single-particle transitions. α_{IB} (full line); α_3, α_4 (broken line); α_1 (dotted line; in this case δE represents position of sharp line rather than a band edge); α_2 (chain line).

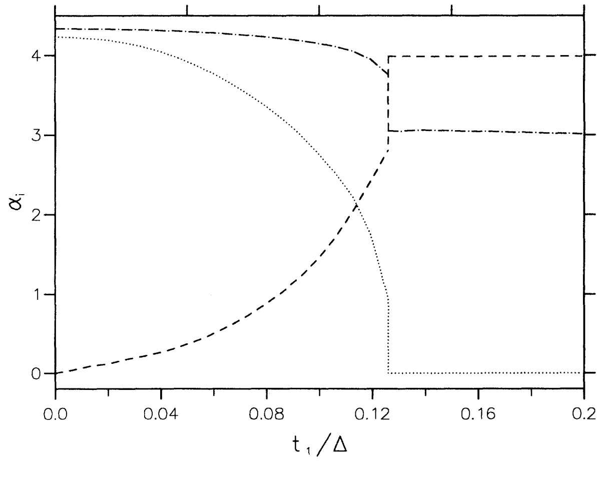

FIG. 13. *Trans*-polyacetylene; $2N+1$ electrons. Absorption coefficients, α_i $(i=1, 2, 4)$ as a function of t_1. Key is as in Fig. 11: α_1 (dotted line); α_2 (chain line); α_4 (broken line). α_3 is precisely double α_4. Absorption is in arbitrary units.

Bishop, and Campbell,[22] who used a continuum model. A value of their parameter ω_0/Δ_0 of 0.71 is appropriate for making the comparison with our (the standard SSH) model; for this value, $\alpha_3+\alpha_4$ is negligible and α_1 and α_2 have similar magnitude.

The most striking feature of Fig. 13 is the reversal of the relative importance of α_1 and α_4 as the interchain coupling is increased. Indeed, when t_1 is strong enough to delocalize the polaron, the sharp line arising from transitions between the gap states has zero intensity. The frequency-dependent absorption within the gap, $\alpha'(\omega)$, is shown in Fig. 14 for three values of the interchain coupling. There are three absorption lines. The one at lowest frequency is α_2; it occurs in each of the figures, it does not vary much in intensity, and it tends to a slightly lower frequency with increasing interchain coupling (consistent with Figs. 11 and 13). The absorption line next above α_2 in frequency is α_1 $(G_L \rightarrow G_U)$. It can be seen that this component decreases in intensity as the coupling increases and disappears altogether when $t_1 > t_{1c}$ in the bottom of the three figures. The third component is $\alpha_3(\omega)+\alpha_4(\omega)$, which is minimal at the smallest value of t_1 in accord with Fig. 13. The interband absorption edge is at $\hbar\omega/\Delta=2$ and so, in practice, the $\alpha_3(\omega)+\alpha_4(\omega)$ component appears as a peak or shoulder on this edge depending on the Gaussian broadening used. The $\alpha'(\omega)$ spectra are relatively insensitive to the chain length [particularly the $\alpha_1(\omega)$ component], while $\alpha_{\mathrm{IB}}(\omega)$ scales roughly with the length of the chain.

These observations have potentially important implications for the interpretation of experimental results. In particular, the line that would correspond to our $\alpha_3(\omega)+\alpha_4(\omega)$ is expected to be much stronger than is predicted by the single-chain SSH theory. Interestingly, Sum, Fesser, and Büttner[23] have shown that a similar effect can be produced by breaking the symmetry of the SSH model by introducing additional electron-phonon coupling.

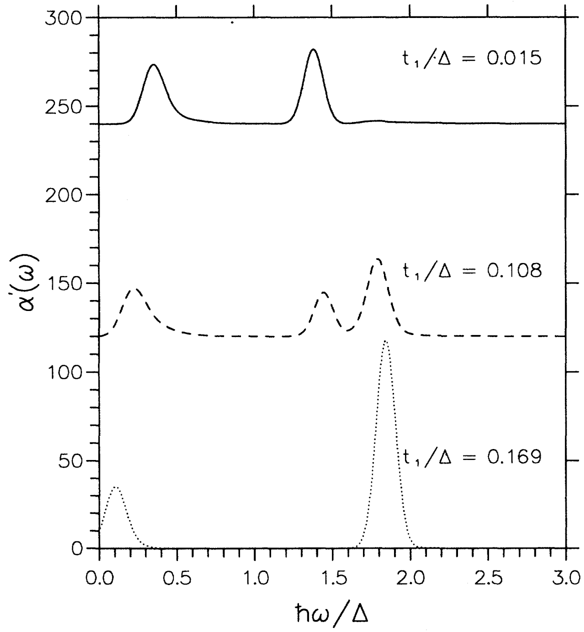

FIG. 14. *Trans*-polyacetylene; $2N+1$ electrons. Components of absorption, $\alpha'(\omega)$, for three values of t_1. Gaussian broadening of 0.06 (in units of Δ) has been used. Absorption is in arbitrary units. Curves have been given a relative vertical displacement of 120 units.

The behavior of α_1 can be understood easily in terms of the "bonding" and "antibonding" nature of the gap states. Let $V^{\pm}_{j,n}$ denote the projection of a state of energy $\pm\epsilon$ onto the π orbital on site n of chain j. Then, from the symmetry of the SSH Hamiltonian,

$$V^{+}_{j,n}=(-1)^{n+j}V^{-}_{j,n} \; . \tag{29}$$

Neglecting the small fluctuating (i.e., u dependent) component in $t^{\pm}_{j,n}$ and $X^{\pm}_{j,n}$, the essential contribution to α_1 can be written

$$\alpha_1(\omega)\sim\sum_{j,n} V^{-}_{j,n}(V^{+}_{j,n+1}-V^{+}_{j,n-1}) \; . \tag{30}$$

Using Eq. (29), this can be expressed as

$$\alpha_1(\omega)\sim\sum_{j,n} -(-1)^{n+j}V^{-}_{j,n}(V^{-}_{j,n+1}-V^{-}_{j,n-1}) \; . \tag{31}$$

If the interchain coupling is zero so that the polaron is confined on one chain (say $j=1$), then $V^{-}_{2,n}=0$. Furthermore, the signs of $V^{-}_{1,n}$ have the pattern $++--++--\cdots$ along the chain so that

$$\operatorname{sgn}V^{-}_{1,n}\operatorname{sgn}V^{-}_{1,n-1}=(-1)^{n} \; . \tag{32}$$

Hence, from Eqs. (31) and (32)

$$\alpha_1(\omega)\sim\sum_{n}|V^{-}_{1,n}|(|V^{-}_{1,n+1}|+|V^{-}_{1,n-1}|) \tag{33}$$

and the contributions to the sum in Eq. (33) are additive and a finite value of $\alpha_1(\omega)$ is obtained in the $t_1\rightarrow 0$ limit.

When there is delocalization of the polaron at large t_1 there is the additional symmetry $V^{-}_{1,n}=V^{-}_{2,n}$. This allows us to write, from Eq. (31),

$$\alpha_1(\omega)\sim\sum_{j,n}-(-1)^{n+j}V^{-}_{1,n}(V^{-}_{1,n+1}-V^{-}_{1,n-1}) \; , \tag{34}$$

and there is cancellation from the summation over the two chains resulting in the vanishing of α_1 as is seen in Figs. 13 and 14.

B. *Trans*-polyacetylene ($2N+2$ electrons)

The discussion for the $2N+2$ electron case differs from that for the single injected electron in a number of respects. The upper gap state G_U, is fully occupied so that the transitions that gave rise to α_1 and to α_4 can no longer occur. $\alpha(\omega)$ and $\alpha'(\omega)$ now receive contributions only from $\alpha_2(\omega)$ and $\alpha_3(\omega)$, and there are, at most, two absorption lines in the gap. In the zero coupling limit, the bipolaron dissociates into a soliton and an antisoliton both associated with electronic states at the center of the gap, and $\alpha_2(\omega)$ and $\alpha_3(\omega)$ are identical. There is a single absorption peak in the center of the gap. As coupling is increased G_U and G_L move apart in energy and two peaks appear.

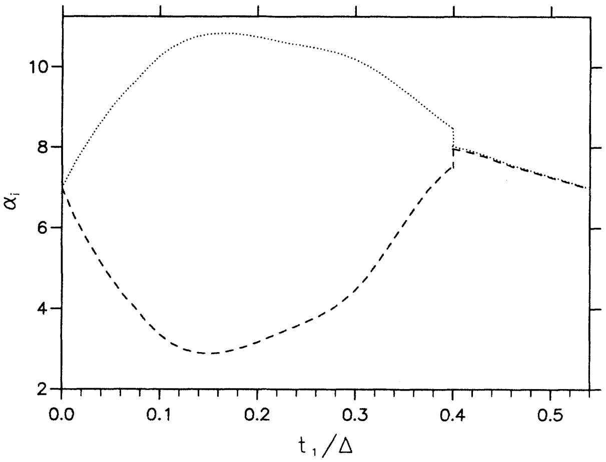

FIG. 15. *Trans*-polyacetylene; $2N+2$ electrons. Absorption coefficients α_i ($i=2$, 3) as a function of t_1. Key: α_2 (dotted line); α_3 (broken line). Absorption is in arbitrary units.

The relative intensity of the two absorption bands is shown in Fig. 15. It can be seen that, for intermediate values of coupling, absorption associated with transitions from the lower of the two gaps states is of lower intensity than that arising from G_U. The absorption components $\alpha'(\omega)$ are shown in Fig. 16. The two peaks are indistinguishable at low t_1 while, for the two higher values, two peaks are clearly apparent. The structure occurring in the upper peak of the bottom figure is a finite-size effect which has not been smoothed out with the width of Gaussian broadening that has been used.

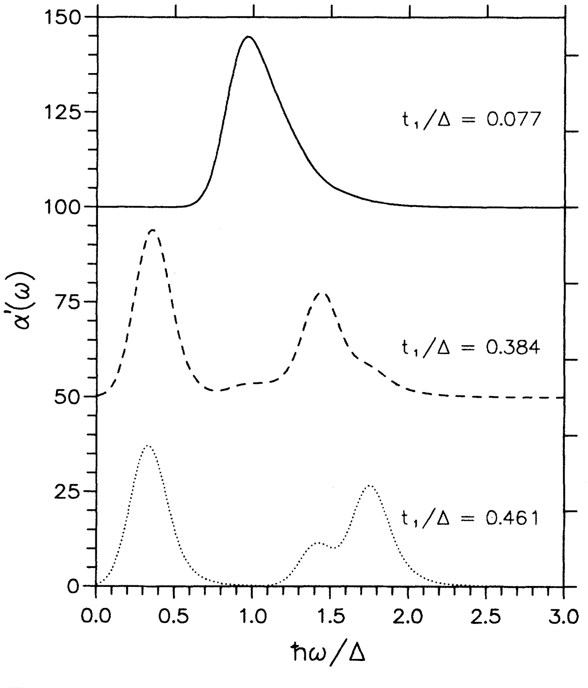

FIG. 16. *Trans*-polyacetylene; $2N+2$ electrons. Components of absorption, $\alpha'(\omega)$, for three values of t_1. Gaussian broadening of 0.11 (in units of Δ) has been used. Absorption is in arbitrary units. Curves have been given a relative vertical displacement of 50 units.

C. *Cis*-polyacetylene ($2N+1$) electrons)

If energies (t_1 and $\hbar\omega$ are scaled by a value of Δ that represents the half-band-gap), then the optical absorption is virtually identical to that displayed in the subsection on *trans*-polyacetylene. The total absorption is close to that shown in Fig. 13 and the spectral dependence is very similar to that displayed in Fig. 14, and so neither is repeated here.

VI. CONCLUSION

The effects of interchain coupling on polaronic and bipolaronic excitations in both degenerate and nondegenerate conjugated polymers have been studied in some detail. For a bipolaron in a nondegenerate polymer, the effect of the coupling is negligible, while for the degenerate *trans*-polyacetylene the soliton-antisoliton pair is stabilized,[24] and for strong coupling, actual delocalization over more than one chain can occur. With just a pair of chains, the coupling energies likely to be encountered in practice are not large enough for complete delocalization to occur (see Fig. 6), but partial delocalization is possible.

The consequences for polaronic excitations are more dramatic. Both degenerate and nondegenerate polymers can be discussed together if energies are scaled by the relevant band gaps (see Figs. 1 and 13, and comments in Secs. IV C and V C). The first point to note is that complete delocalization occurs for interchain coupling that is little more than 10% of the half-band-gap. Band gaps are typically in the (2–3)-eV range and coupling is quoted as being in the region from 0.025–0.1 eV. The calculations reported here were done on a pair of chains. With a full three-dimensional environment, the effects described are likely to occur at even smaller values of interchain coupling and so delocalization (either complete or partial) has to be regarded as a serious possibility.

It should be noted that the incipient three-dimensional polaron that we have explored here is different from that studied by Baeriswyl and Maki[8] (see also analogous work[25] on solitons in two dimensions). Baeriswyl and Maki consider a set of polarons, one per chain, and study the formation of a band of polaron states. The extra electron goes into the lowest state in the upper polaron band. In our work, there is just a single pair of gap states whether or not delocalization has taken place. In other words, the lattice adjusts itself so that the electronic states in the gap can accommodate one added electron (or two for the bipolaron) without the appearance of additional unoccupied gap states. The model we study has relevance to the weak doping regime, whereas a polaron band model may be appropriate in another regime. It would be of interest now to study the polaron confinement in a full three-dimensional environment. The delocalized polaron will spread over several chains forming a highly anisotropic excitation.

There have been a large number of experimental studies into the nature of the excited states in polymers formed either during photoexcitation or following doping. ESR and optical-absorption measurements are the principal tools used to distinguish polarons from bipolarons. The materials most studied over the last decade have been polythiophene[26–32] and polypyrrole.[32–35] Some of the work[30,31,36] reports on bipolarons as the completely dominant excitation, while others regard the polaron as important at low doping levels (typically below 1% concentration) but with the bipolarons predominating at high levels of doping. There are some reports[29,33] of three absorption peaks associated with the polaron states; this is in disagreement with standard theoretical models which predict two peaks but, from the present work, it would be the expected outcome for intermediate values of interchain coupling.

The interpretation of experimental data is complicated by the fact that the injected electrons or holes are introduced by electrochemical doping. The doping itself can possibly inhibit bipolaron formation, and it has been suggested[26] that, in addition to shallow polarons of the type discussed here, there can also be present deep polaron states associated with the defects. The role of the Coulomb interaction also has to be considered and here there are contradictory estimates of its importance. More recent work[35,37] indicates that the polaron may play an important role at intermediate or high doping levels through the formation of a polaron band or lattice.

The present work indicates that interchain coupling is likely to play a significant role in the behavior of polaronic excitations and will be important in any interpretation of optical data. Its effect on bipolarons in nondegenerate polymers appears to be negligible, but in a degenerate system, of course, it plays a vital role in soliton confinement.

ACKNOWLEDGMENTS

One of us (M.K.S.) acknowledges the support of the Syrian Atomic Energy Commission during the course of this work. The authors also acknowledge useful discussions with Dr. G. R. Mitchell of the Reading University Polymer Science Centre.

---

[*] Present address: P.O. Box 6091, Damascus, Syria.

[1] W. P. Su, J. R. Schrieffer, and A. J. Heeger, Phys. Rev. B **22**, 2099 (1980); **28**, 1138(E) (1983).

[2] A. J. Heeger, S. Kivelson, J. R. Schrieffer, and W. P. Su, Rev. Mod. Phys. **60**, 781 (1988).

[3] P. L. Danielsen and R. C. Ball, J. Phys. (Paris) **46**, 131 (1983).

[4] D. Baeriswyl and K. Maki, Phys. Rev. B **28**, 2068 (1983).

[5] H. Kahlert, A. Leitner, and G. Leising, Synth. Met. **17**, 467 (1987).

[6] D. Baeriswyl and K. Maki, Phys. Rev. B **38**, 8135 (1988).

[7] J. A. Blackman and M. K. Sabra, Polymer **31**, 621 (1990).

[8] D. Baeriswyl and K. Maki, Synth. Met. **28**, D507 (1989).

[9] Y. N. Gartstein and A. A. Zakhidov, Solid State Commun. **62**, 213 (1987).

[10] Y. N. Gartstein and A. A. Zakhidov, Synth. Met. **28**, D501 (1989).

[11] C. R. Fincher, Jr., C.-E. Chen, A. J. Heeger, and A. G. MacDiarmid, Phys. Rev. Lett. **48**, 100 (1982).

[12] K. Shimamura, F. E. Karasz, J. A. Hirsch, and J. C. W. Chien, Macromol. Chem. **2**, 473 (1981).

[13] S. Jeyadev, Phys. Rev. B **28**, 3447 (1983).

[14] S. Stafström, Phys. Rev. B **32**, 4060 (1985).

[15] D. Emin, Phys. Rev. B **33**, 3973 (1986).

[16] M. Takayama, Y. R. Lin-Liu, and K. Maki, Phys. Rev. B **21**, 2388 (1980).

[17] S. A. Brazovskii and N. Kirova, Pis'ma Zh. Eksp. Teor. Fiz. **33**, 6 (1981) [JETP Lett. **33**, 4 (1981)].

[18] C. L. Wang, Z. B. Su, and F. Martino, Phys. Rev. B **33**, 1512 (1986).

[19] G. Leising, Phys. Rev. B **38**, 10 313 (1988).

[20] G. D. Mahan, *Many-Particle Physics* (Plenum, New York, 1981), p. 31.

[21] J. T. Gammel and J. A. Krumhansl, Phys. Rev. B **24**, 1035 (1981).

[22] K. Fesser, A. R. Bishop, and D. K. Campbell, Phys. Rev. B **27**, 4804 (1983).

[23] U. Sum, K. Fesser, and H. Büttner, Phys. Rev. B **38**, 6166 (1988).

[24] There have been a number of other discussions relating to this issue: D. Bertho, J. P. Albert, and C. Jouanin, Mol. Cryst. Liq. Cryst. **117**, 209 (1985); K. Maki, *ibid.* **117**, 213 (1985); Ref. 7.

[25] K. Fesser, Synth. Met. **25**, 1 (1988).

[26] K. Kaneto, Y. Kohno, and K. Yoshino, Solid State Commun. **51**, 267 (1984).

[27] T. Hattori, W. Hayes, K. Wong, K. Kaneto, and K. Yoshino, J. Phys. C **17**, L803 (1984).

[28] G. Harbeke, E. Meier, W. Kobel, M. Egli, H. Kiess, and E. Tosatti, Solid State Commun. **55**, 419 (1985).

[29] G. Harbeke, D. Baeriswyl, H. Kiess, and W. Kobel, Phys. Scr. **T13**, 302 (1986).

[30] Z. Vardeny, E. Ehrenfreund, O. Brafman, M. Nowak, H. Schaffer, A. J. Heeger, and F. Wudl, Phys. Rev. Lett. **56**, 671 (1986).

[31] N. Colaneri, M. Nowak, D. Spiegel, S. Hotta, and A. J. Heeger, Phys. Rev. B **36**, 7964 (1987).

[32] Y. Yumoto, K. Morishita, and S. Yoshimura, Synth. Met. **18**, 203 (1987).

[33] K. Yakushi, L. J. Lauchlan, T. C. Clarke, and G. B. Street, J. Chem. Phys. **79**, 4774 (1983); J. L. Brédas, J. C. Scott, K. Yakushi, and G. B. Street, Phys. Rev. B **30**, 1023 (1984).

[34] F. Genoud, M. Guglielmi, M. Nechtsschein, E. Genies, and M. Salmon, Phys. Rev. Lett. **55**, 118 (1985).

[35] P. Bätz, D. Schmeisser, and W. Göpel, Solid State Commun. **74**, 461 (1990).

[36] D. D. C. Bradley, R. H. Friend, and W. J. Feast, Synth. Met. **17**, 645 (1987).

[37] S. Tabor and S. Stafström, Phys. Rev. B **44**, 12 737 (1991).